

Full Paper

## Performance of self-excited induction generator with cost-effective static compensator

Yogesh K. Chauhan<sup>1,\*</sup>, Sanjay K. Jain<sup>2</sup> and Bhim Singh<sup>3</sup>

<sup>1</sup> Department of Electrical Engineering, School of Engineering, Gautam Buddha University, G.B. Nagar-201310, India

<sup>2</sup> Electrical and Instrumentation Engineering Department, Thapar University, Patiala-147004, India

<sup>3</sup> Department of Electrical Engineering, Indian Institute of Technology, New Delhi-110016, India

\* Corresponding author, e-mail: [chauhanyk@yahoo.com](mailto:chauhanyk@yahoo.com)

Received: 6 June 2010 / Accepted: 8 January 2012 / Published: 13 January 2012

---

**Abstract:** The performance of a system consisting of a three-phase self-excited induction generator (SEIG) with static compensator (STATCOM) for feeding static resistive-inductive (R-L) and dynamic induction motor (IM) loads was investigated. The cost-effective STATCOM providing stable operation was designed by connecting additional shunt capacitance with the load. The STATCOM-controlled algorithm was realised by controlling the source current using two control loops with proportional-integral (PI) controller: one for controlling the SEIG terminal voltage and the other for maintaining the DC bus voltage. The SEIG-STATCOM performance was studied for two designs of STATCOM, namely cost-effective STATCOM and full-rating STATCOM. The cost-effective SEIG-STATCOM system with the proposed control scheme exhibited improved performance with respect to starting time, voltage dip, generator current and total harmonic distortion under various transient conditions.

**Keywords:** self-excited induction generator (SEIG), static compensator (STATCOM), voltage regulation, renewable energy source

---

### INTRODUCTION

The fast rate of fossil fuel depletion is drawing attention to explore the alternative energy sources, e.g. small hydropower, wind and tidal power [1, 2]. The induction generator [3, 4] which operates in grid or self-excited mode is a strong candidate to harness electrical energy from these

sources. An isolated electric supply using a self-excited induction generator (SEIG) is an economical option for such small-capacity applications as lighting and small motor loads in remote locations.

The SEIG consists of a cage induction machine excited through an externally connected capacitor bank. The primary advantages of the SEIG in small capacity are the simple, brush-less and rugged construction, lower maintenance cost, small size and improved transient performance. The terminal voltage of SEIG is governed by parameters such as capacitance, prime mover speed and speed-torque characteristic and load. A poor voltage regulation results when the SEIG is loaded [5, 6] due to the increasing difference between the volt-ampere reactive (VAR) supplied by the capacitor bank and that demanded by the generator and load. The series capacitors [7-9] have been used with the SEIG for improved voltage regulation. The application of a thyristor as a static switch has resulted in such schemes as saturable core reactors and switching shunt capacitors for achieving improved voltage regulation of SEIG [10-12].

The modern power electronic converters are characterised by fast response, improved switching features and low cost. These converters are being applied as flexible alternating current transmission systems (FACTS) for various control and regulating purposes. The performance and cost of the shunt capacitor, static VAR compensator (SVC) and STATCOM were compared [13]. The STATCOM is normally a current controlled-voltage source inverter (CC-VSI) and has wide applications in the power system for improving power quality, harmonic elimination, reactive power compensation and load balancing [14,15]. The installation issue and capability of STATCOM have been demonstrated for the voltage limited feeder and industrial facility [16,17]. The concepts of static compensation for SEIG have been described for static loads [18,19]; the steps in designing a STATCOM for SEIG system have been summarised [20]. However, most of these attempts have been made to feed three-phase static loads and very little efforts are made for SEIG feeding the dynamic (motor) loads.

In this paper, the performance of SEIG with STATCOM on feeding a static R-L load and induction motor is investigated. The dynamic model of the system is developed and a methodology to decide the ratings of STATCOM components such as the DC bus capacitor, AC side filter and insulated gate bipolar transistors (IGBT) is presented. The system performance is also studied for cost-effective STATCOM and full-rating STATCOM designs.

## **SYSTEM DESCRIPTION AND CONTROL SCHEME**

The schematic description of the SEIG-STATCOM system is shown in Figure 1. A suitable capacitor bank is needed to obtain the rated voltage at no load. The STATCOM consists of an IGBT-based 3- $\phi$  CC-VSI, an AC side-filter inductor, and a capacitor on the self-supporting DC bus. The scheme to control the STATCOM is depicted in Figure 2. In this scheme, two control loops are employed: one for controlling the terminal voltage of SEIG and other for maintaining the DC bus voltage. The proportional-integral (PI) controller is used with both control loops, which possess the advantage of being simple, effective and easy to tune.

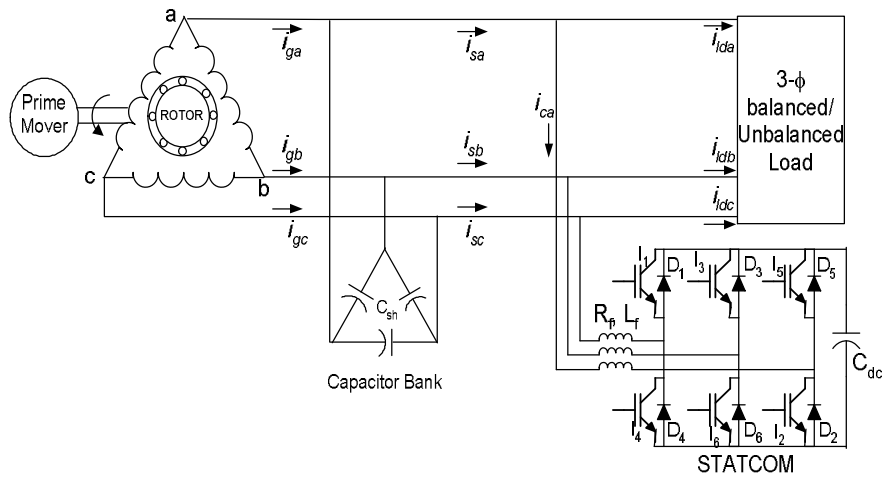


Figure 1. SEIG-STATCOM system supplying the load

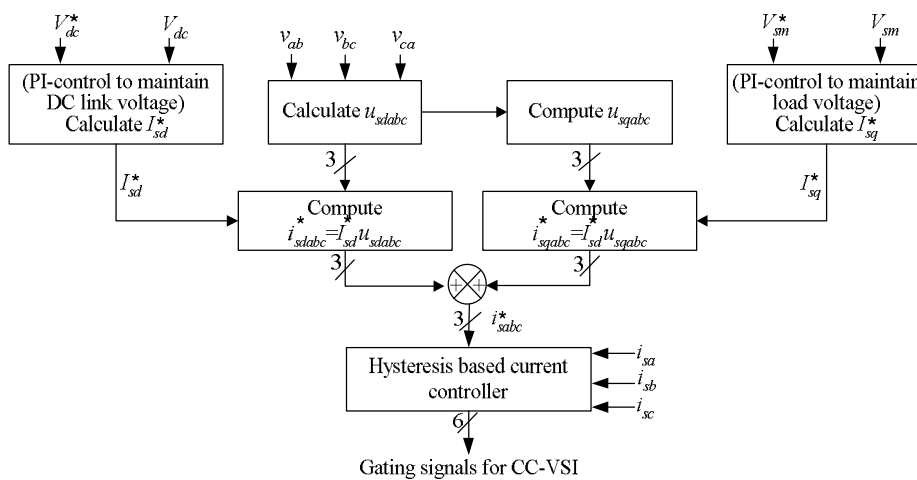


Figure 2. Control scheme for STATCOM

The control scheme is based on direct control of the source current, which consists of in-phase  $I_{sd}^*$  and quadrature  $I_{sq}^*$  components.  $I_{sd}^*$  is the current drawn from SEIG to maintain the DC bus voltage by charging (or discharging) the DC bus capacitor.  $I_{sq}^*$  is the reactive current required to maintain the SEIG terminal voltage. To regulate the DC bus voltage, the error signal for the PI controller is obtained from the sensed DC bus voltage  $V_{dc}$  and its reference value  $V_{dc}^*$ . The output of this PI controller is taken as  $I_{sd}^*$ . The 3- $\phi$  reference in-phase current  $i_{sdabc}^*$  is obtained by multiplying  $I_{sd}^*$  with the sinusoidal in-phase unit voltage template  $u_{sdabc}$ . To regulate the SEIG terminal voltage, the error signal for PI controller is obtained from the amplitude of SEIG voltage  $V_{sm}$  and its reference value  $V_{sm}^*$ . The output of this PI controller is taken as  $I_{sq}^*$ . The 3- $\phi$  reference quadrature current  $i_{sqabc}^*$  is obtained by multiplying  $I_{sq}^*$  with the sinusoidal quadrature unit voltage template  $u_{sqabc}$ . The total reference source current  $i_{sabc}^*$  is taken as the sum of  $i_{sdabc}^*$  and  $i_{sqabc}^*$ . The sensed and reference source currents are processed in a rule based carrier less hysteresis band current controller to generate gating signals ( $S_a, S_b, S_c$ ) for IGBT of CC-VSI of STATCOM.

## DESIGN METHODOLOGY

The STATCOM is designed considering that the VAR rating of STATCOM is fixed, the source voltage is completely sinusoidal and the pulse width modulation (PWM) inverter operates in linear mode. The VAR rating of STATCOM,  $(VAR)_{STATCOM}$ , is estimated using the capacitance needed for providing the rated voltage at no load ( $C_{NL}$ ) and that needed for a stable operation of the induction motor while being loaded to its rated capacity ( $C_{FL}$ ). These capacitances are computed using sequential unconstrained minimisation technique (SUMT) in conjunction with Rosenbroack's direct search method [23]. The problem formulation is briefed in Appendix I. The  $(VAR)_{STATCOM}$  is computed as

$$(VAR)_{STATCOM} = 3V_{ab}^2 \left[ \frac{1}{X_{C_{FL}}} - \frac{1}{X_{C_{NL}}} \right] \quad (1)$$

and STATCOM line current  $I_{st}$  is calculated as

$$I_{st} = \frac{(VAR)_{STATCOM}}{\sqrt{3}V_{ab}} \quad (2)$$

The reference DC bus voltage  $V_{dcr}$  of the voltage source converter of STATCOM depends upon the AC voltage. The STATCOM does not provide adequate compensation during the transient condition of low  $V_{dcr}$ , whereas high  $V_{dcr}$  may stress the devices. The  $V_{dcr}$  is calculated using the peak supply line voltage  $V_m$  [15] as

$$V_{dcr} = (1.2-2.0)V_m, \quad V_{dcr} > V_m \quad (3)$$

The DC bus capacitor  $C_{dc}$  stores energy and maintains the DC bus voltage with small ripple. The  $C_{dc}$  is calculated using an energy balanced equation characterised by appropriate response time  $t$  and actual DC bus voltage  $V_{dca}$ :

$$C_{dc} = \frac{\sqrt{3}V_{ab}I_{st}t}{\{V_{dcr}^2 - V_{dca}^2\}} \quad (4)$$

The AC filter inductance  $L_f$  is decided by the allowable ripple in the compensation current [20].  $L_f$  is calculated by assuming a linear mode operation (modulation index  $m=1$ ) and a switching frequency  $f_s$  of 10 kHz:

$$L_f = \frac{\left(\frac{\sqrt{3}}{2}\right)V_{dc}}{6af_s K_{rp}} \quad (5)$$

where the range of factor  $a$  (transient current) = 1.2-2.0 and  $K_{rp}$  (peak-to-peak ripple) = 0.05-0.1.

The ratings of IGBT suitable for medium rating and high frequency operation are decided as follows:

$$\begin{aligned} V_{dev} &= (1 + K_L + K_t)V_m \\ I_{dev} &= \sqrt{2}K_s(K_{rp} + 1)I_{st} \end{aligned} \quad (6)$$

where the ranges of  $K_L$  (factor for filter inductor drop),  $K_t$  (factor for transient voltage) and  $K_s$  (factor of safety) are taken as 0.05-0.1, 0.1-0.2 and 1.25-1.50 respectively.

## SYSTEM MODEL

The complete system as shown in Figure 1 consists of SEIG, STATCOM with associated control, and loads. The dynamic model of each component is presented herewith.

### SEIG Model

The induction generator model is developed in a stationary q-d reference frame considering the effect of both main and cross flux saturation [21, 22]. The model, i.e. the q-d axis stator and rotor currents and the rotor speed ( $\omega_r$ ), in state space form is expressed using equations (7) and (8) respectively:

$$p[i] = [L]^{-1}([v] - [r][i] - [G][i]) \quad (7)$$

$$p\omega_r = \frac{P}{2J}(T_p - T_{em}) \quad (8)$$

where  $T_{em} = \frac{3P}{4}L_m(i_{qs}i_{dr} - i_{ds}i_{qr})$ , and  $[v]$ ,  $[i]$ ,  $[r]$ ,  $[L]$ ,  $[G]$  and  $T_p$  are defined in Appendix-II.

### Shunt Capacitor Model

The q-d axis stator currents  $i_{qs}$  and  $i_{ds}$  are converted into 3- $\phi$  stator currents  $i_{ga}$ ,  $i_{gb}$  and  $i_{gc}$  using 2- $\phi$  to 3- $\phi$  transformation [22]. Kirchhoff's current law (KCL) [22] is applied to obtain the capacitor equations governing the SEIG voltage as

$$pv_{ab} = \frac{\{(i_{ga} - i_{lda} - i_{ca}) - (i_{gb} - i_{ldb} - i_{cb})\}}{3C_{sh}} \quad (9)$$

$$pv_{bc} = \frac{\{(i_{ga} - i_{lda} - i_{ca}) + 2(i_{gb} - i_{ldb} - i_{cb})\}}{3C_{sh}}$$

$$\text{and } v_{ab} + v_{bc} + v_{ca} = 0 \quad (10)$$

where  $i_{ga}$ ,  $i_{lda}$  and  $i_{ca}$  are line 'a' currents for the generator, load and STATCOM respectively.

### STATCOM Model

The charging (or discharging) of the DC bus capacitor  $C_{dc}$  using hysteresis current controller switching functions ( $S_a$ ,  $S_b$ ,  $S_c$ ) is expressed as

$$pV_{dc} = \frac{(i_{ca}S_a + i_{cb}S_b + i_{cc}S_c)}{C_{dc}} \quad (11)$$

The DC bus voltage  $V_{dc}$  is reflected as voltages  $e_a$ ,  $e_b$  and  $e_c$  on the AC side of the PWM inverter as

$$\begin{bmatrix} e_a \\ e_b \\ e_c \end{bmatrix} = \frac{V_{dc}}{3} \begin{bmatrix} 2 & -1 & -1 \\ -1 & 2 & -1 \\ -1 & -1 & 2 \end{bmatrix} \begin{bmatrix} S_a \\ S_b \\ S_c \end{bmatrix} \quad (12)$$

The AC side filter equations in state space form are expressed as

$$\begin{aligned}
 p i_{ca} &= \frac{\{(v_{bc} + 2v_{ab}) - (e_{bc} + 2e_{ab}) - 3R_f i_{ca}\}}{3L_f} \\
 p i_{cb} &= \frac{\{(v_{bc} - v_{ab}) - (e_{bc} - e_{ab}) - 3R_f i_{cb}\}}{3L_f}
 \end{aligned} \tag{13}$$

where  $e_{ab} = e_a - e_b$  and  $e_{bc} = e_b - e_c$ .

### Static R-L Load

The static load is considered as delta-connected. The phase currents for static R-L load ( $i_{prla}$ ,  $i_{prlb}$  and  $i_{prlc}$ ) are expressed as

$$\begin{aligned}
 p i_{prla} &= (v_{ab} - R_a i_{prla}) / L_a \\
 p i_{prlb} &= (v_{bc} - R_b i_{prlb}) / L_b \\
 p i_{prlc} &= (v_{ca} - R_c i_{prlc}) / L_c
 \end{aligned} \tag{14}$$

Correspondingly, the line currents ( $i_{rla}$ ,  $i_{rlb}$  and  $i_{rlc}$ ) can be obtained as follows:

$$\begin{aligned}
 i_{rla} &= (i_{prla} - i_{prlc}) \\
 i_{rlb} &= (i_{prlb} - i_{prla}) \\
 i_{rlc} &= (i_{prlc} - i_{prlb})
 \end{aligned} \tag{15}$$

### Induction Motor Load

The values for  $v_{qs}$  and  $v_{ds}$  are obtained from SEIG voltages ( $v_{ab}$ ,  $v_{bc}$ ,  $v_{ca}$ ) using 3- $\phi$  to 2- $\phi$  transformation [22]. The state space model of an induction motor dynamic load is similar to the induction generator model. It is expressed using motor parameters as

$$p [i_m] = [L_m]^{-1} ([v_m] - [r_m] [i_m] - [G_m] [i_m]) \tag{16}$$

$$p \omega_{rm} = \frac{P_m}{2J_m} (T_{emm} - T_L) \tag{17}$$

The equations (7-17) represent the model of the complete system. These equations are solved by fourth-order Runge-Kutta integration method [22] in MATLAB.

## RESULTS AND DISCUSSION

An investigation was carried out on a 3.7-kW induction machine operated as SEIG, which was loaded with a static R-L load of 0.8 pf and a 1.5-kW induction motor load. The parameters of this machine are given in Appendix III. The capacitances  $C_{NL}$  and  $C_{FL}$  were calculated as 16.1  $\mu F$  and 26.5  $\mu F$  respectively for the rated SEIG voltage at no load and at the rated motor load under steady state.

It was observed that the motor was unable to start even with  $C_{FL}$  and resulted in a voltage collapse because the capacitor bank was unable to meet the excessive VAR requirements of SEIG and the motor load during starting. The starting of the motor was successful with a capacitance of 36  $\mu F$ . The performance during voltage buildup, the starting of motor at 2.0 sec., and the subsequent loading on motor at 4.0 sec. are shown in Figure 3. During starting, the terminal voltage dropped to 0.25 p.u. and the induction motor took 0.7 sec. to stabilise the start-up transients. The excessive dip in voltage level and the longer duration for start-up were of serious quality concern. In addition, the SEIG exhibited poor voltage regulation even for the static load.

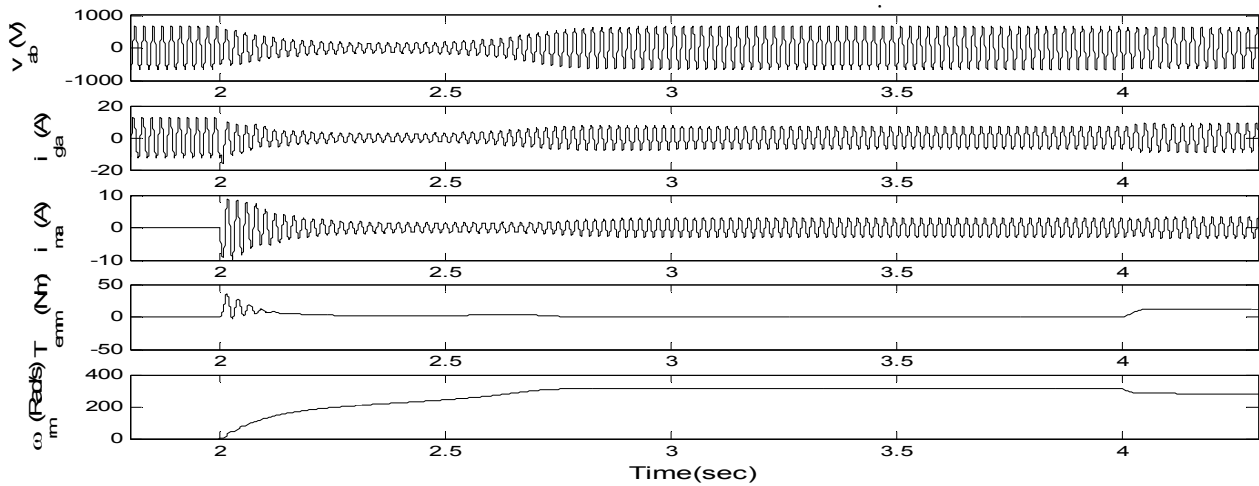


**Figure 3.** SEIG feeding motor load with successful starting and consequent loading  
(Load conditions: 1.5-kW induction motor load at 2.0 sec. with  $C_{sh} = 36 \mu F$ )

The application of STATCOM was investigated for effective control and improved performance. The STATCOM was designed to give a cost-effective operation by selecting the  $C_{dc}$  after considering the VAR requirement carefully. For a cost-effective STATCOM, the required VAR rating of STATCOM was calculated using the limiting capacitance of  $C_{NL}$  and  $(C_{FL} + C_{NL})/2$  while an additional  $(C_{FL} - C_{NL})/2$  shunt capacitance was switched on with the load. For a full-rating STATCOM, the VAR rating of STATCOM was calculated with limiting capacitances  $C_{NL}$  and  $C_{FL}$ . For both the cost-effective and full-rating STATCOM designs, the shunt capacitance  $C_{NL}$  needed to achieve the rated SEIG voltage at no load was taken as  $16.1 \mu F$ . The different values of  $C_{FL}$  were obtained for the static and motor loads.

The capacitance needed for successful starting of the induction motor, which was  $36 \mu F$ , was taken as  $C_{FL}$  for the motor load.  $C_{FL}$  for the static load was considered as the capacitance needed to obtain the rated voltage at steady state, which was  $30.4 \mu F$ . The STATCOM parameters are summarised in Table 1 for both cost-effective and full-rating STATCOM designs. The IGBT of reduced current ratings were needed for a cost-effective STATCOM, which reduced the cost, and therefore the operation should be cost-effective.

**Table 1.** STATCOM design parameters

Parameter	Cost-effective STATCOM		Full-rating STATCOM	
	2.2kW static load (0.8 pf)	1.5 kW IM load	2.2kW static load (0.8 pf)	1.5 kW IM load
STATCOM rating	1.21 kVAR	1.615 kVAR	2.42 kVAR	3.23 kVAR
Current supplied by STATCOM	1.68 A	2.25 A	3.37 A	4.5 A
Ref. DC bus voltage	700 V	700 V	700 V	700 V
DC bus capacitance	86.3 $\mu F$	118.1 $\mu F$	172.6 $\mu F$	236.3 $\mu F$
AC filter inductance	11.16 mH	8.16 mH	5.58 mH	4.08 mH
Device selection	IGBT	IGBT	IGBT	IGBT
Device voltage rating	1094 V	1094 V	1094 V	1094 V
Device current rating	5.5 A	7.5 A	11.0 A	15.0 A

On the basis of STATCOM design parameters, a comparison between the cost-effective and full rating STATCOM is summarised in Table 2.

**Table 2.** Comparison of performance parameters for cost-effective and full-rating STATCOM

Performance parameter	Cost-effective STATCOM	Full-rating STATCOM
Performance (voltage regulation, starting time, THD, etc.)	Reasonably good	Good
Energy consumption (mainly in IGBT, DC bus capacitor and filter inductor loss)	Low (lower IGBT current rating, lower DC bus capacitance and higher filter inductor)	High (higher IGBT current rating, higher DC bus capacitance and lower filter inductor)
Overall cost (IGBT, DC bus capacitor, filter inductor)	Low	High

### Performance with Balanced Static R-L Load

The performance characteristics of the systems with cost-effective and full-rating STATCOM are shown in Figure 4 and Figure 5 respectively for feeding balanced 0.8-pf static R-L load. A load of 2.2 kW was applied at 2.5 sec., which was changed to 3.0 kW at 3.0 sec. and 2.2 kW at 3.5 sec.

With cost-effective STATCOM (Figure 4), the visible transients lasting for about 0.2 sec were observed in  $v_{ab}$ ,  $i_{ga}$  and  $V_{dc}$  due to the application of 2.2-kW load. The  $V_{dc}$  momentarily decreased to 480V and varied between 480-800V before returning to the reference value. With full-rating STATCOM (Figure 5), the transients settled down after 5-6 cycles and the DC bus voltage decreased to 500V momentarily with the application of 2.2-kW load. The increase in static load to 3.0 kW at 3.0 sec. did not result in any appreciable transients due to the choice of  $C_{dc}$  corresponding to the motor load. In both cost-effective and full-rating STATCOM,  $V_{dc}$  dropped momentarily to 630V and gradually returned to the reference value with the PI controller action. When the load was reduced to 2.2 kW at 3.5 sec., the dynamics of the system changed accordingly.  $V_{dc}$  momentarily rised to 760V before returning to the reference mark. A steady state was achieved within 0.12 sec. and 0.25 sec. with the full-rating and cost-effective STATCOM respectively.

### Performance with Unbalanced Static R-L Load

The system performance with the cost-effective STATCOM was studied for an unbalanced R-L load and the corresponding characteristics for three-phase generator voltage  $v_{abc}$ , generator current  $i_{gabc}$ , load current  $i_{rlabc}$ , compensation current  $i_{cabc}$ , and DC bus voltage  $V_{dc}$  are shown in Figure 6. Initially, the 2.2-kW, 3.0-kW and 1.0-kW loads of 0.8 pf were applied on 'a', 'b' and 'c' phases respectively at 3.0 sec. Further, an acute unbalance was made by unloading of 'c' phase at 3.5 sec. The STATCOM responded satisfactory during the unbalanced load condition and maintained the balanced condition at SEIG terminals.



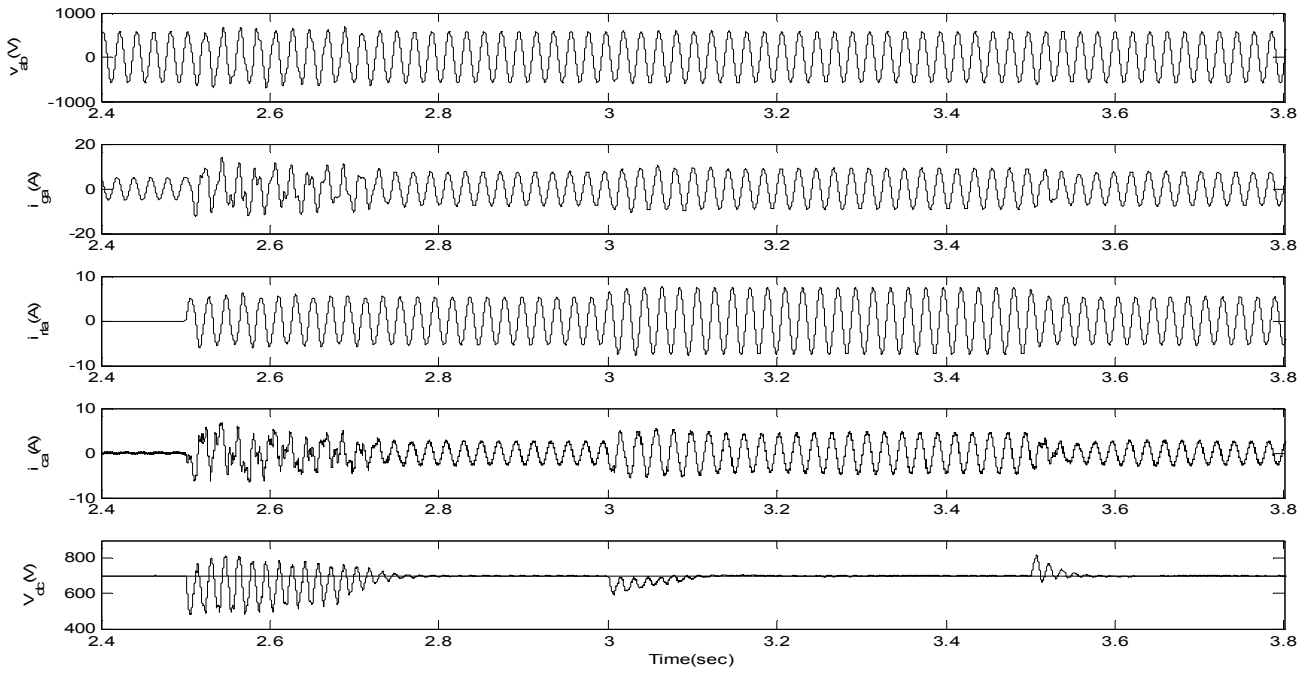


**Figure 4.** Performance characteristics of SEIG-STATCOM (cost-effective) system with 0.8-pf static R-L load (Load conditions : 2.2 kW at 2.5 sec., 3.0 kW at 3.0 sec. and 2.2 kW at 3.5 sec.)

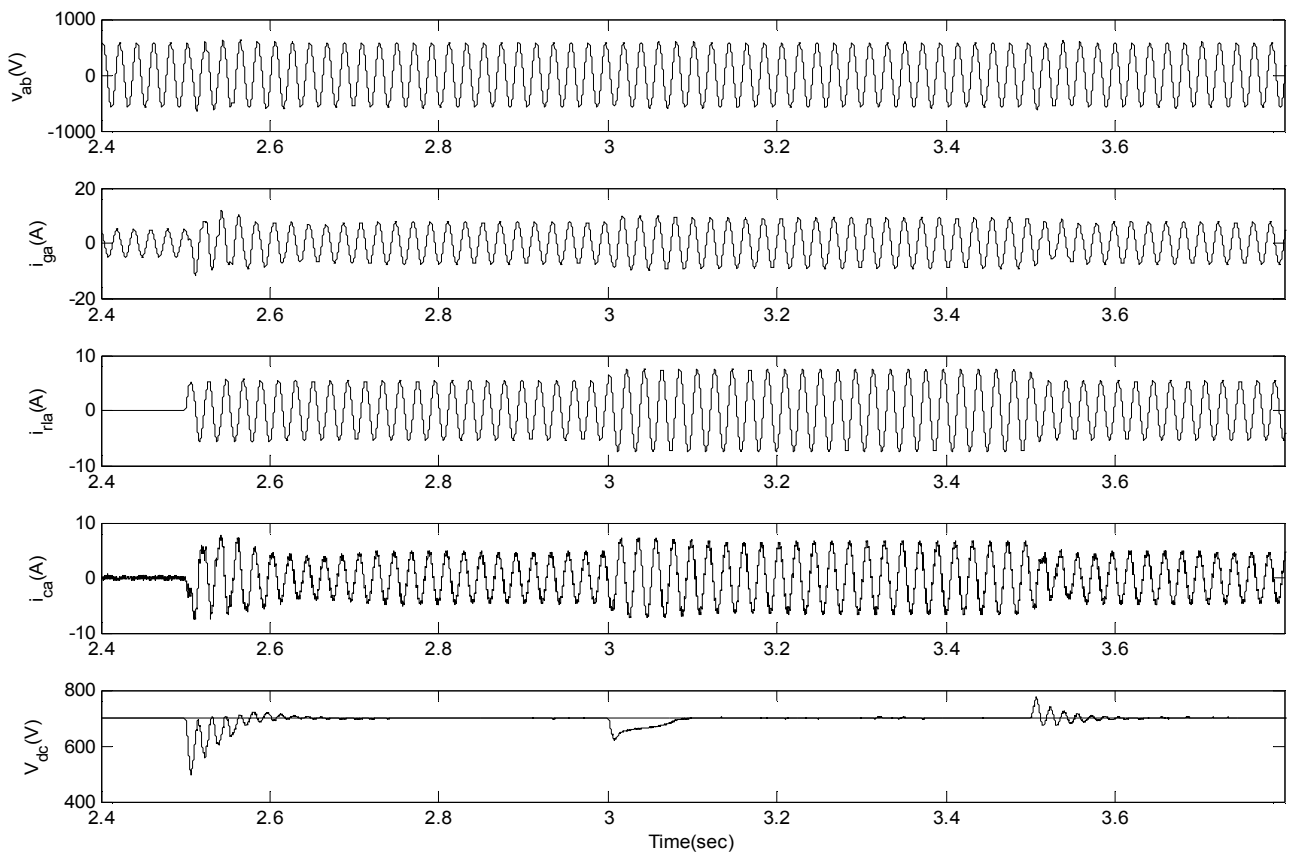


**Figure 5.** Performance characteristics of SEIG-STATCOM (full rating) with 0.8-pf static R-L load (Load conditions: 2.2 kW at 2.5 sec., 3.0 kW at 3.0 sec., and 2.2 kW at 3.5 sec.)

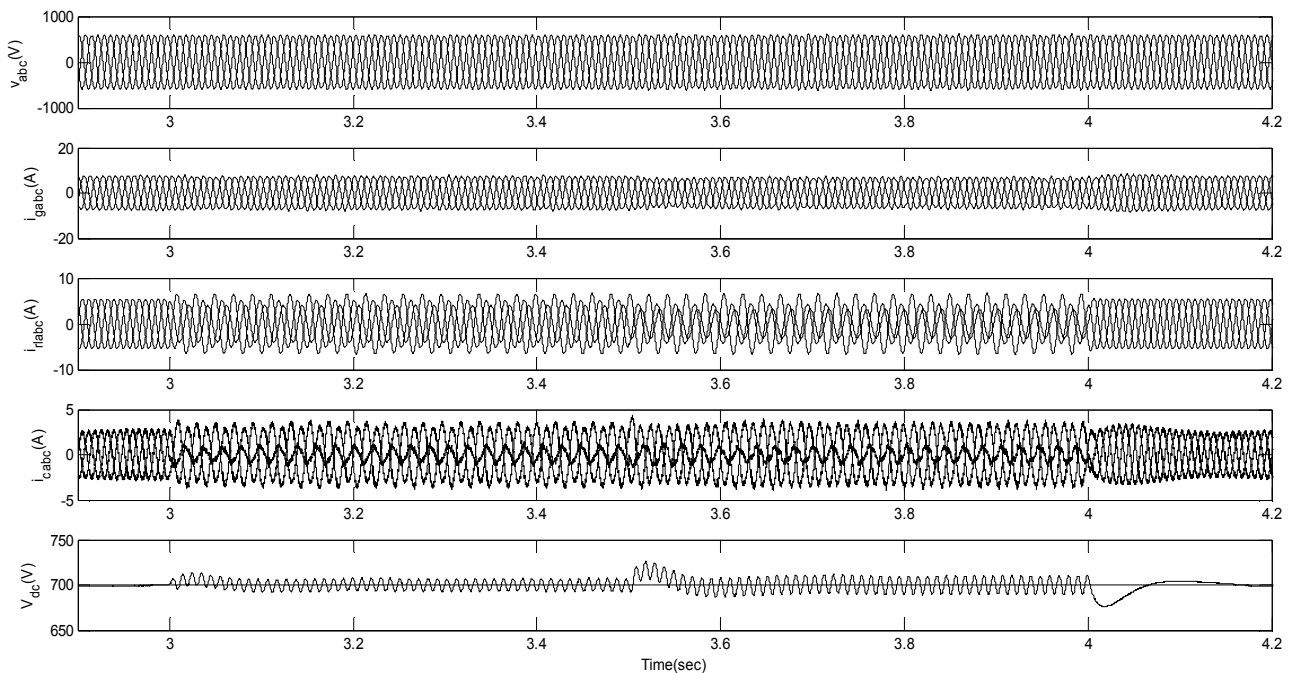


**Figure 6.** Performance characteristics of SEIG-STATCOM (cost-effective) with unbalanced 0.8-pf R-L load (Load conditions: 3- $\phi$  load (2.2 kW, 3.0 kW, 1.0 kW) at 3.0 sec.; load (2.0 kW, 3.0 kW, unloading on 'c' phase) at 3.5 sec; and balanced 3- $\phi$  loading of 2.2.0 kW at 4.0 sec.)

### Performance with Motor Load

The performance characteristics of the system during the starting and sudden loading of an induction motor are shown in Figures 7 and 8 for cost-effective and full-rating STATCOM respectively. The motor at no load was switched on at 3.0 sec. and was loaded at 4.0 sec. During the starting of the motor, excessive reactive VAR were drawn and therefore the  $V_{dc}$  dropped to 300V level with both STATCOM. The  $V_{dc}$  quickly rose above the reference 700V before returning to reference level after replenishing the charge on DC bus capacitor. At starting, the transients in  $v_{ab}$ ,  $i_{ga}$ ,  $i_{ma}$ ,  $T_{emm}$  and  $V_{dc}$  were more visible with cost-effective STATCOM due to its lower rating and the uncharged capacitor connection across the motor load terminals. Because of a lower compensation level, the  $i_{ca}$  under steady state was lower compared to the corresponding value with full-rating STATCOM. With cost-effective STATCOM, the SEIG voltage decreased by 10% and the transients were settled in 0.5 sec., whereas these values were 6% and 0.4 sec. respectively for full-rating STATCOM. Without STATCOM, as shown in Figure 3, the decrease in SEIG voltage was 30%. The motor was loaded with rated load torque at 4.0 sec. After small transients, the system response changed accordingly. The increase in  $i_{ga}$ ,  $i_{ma}$ , and  $T_{emm}$  and the decrease in  $\omega_{rm}$  were observed. The  $V_{dc}$  decreased to 670V before returning to steady-state reference value of 700V.

The performance of SEIG-IM configuration was compared in the presence and absence of STATCOM and the key parameter indices of the system are summarised in Table 3. The total harmonic distortion (THD) was obtained through fast Fourier transform (FFT) using discrete Fourier transform (DFT) algorithm of MATLAB. The generator-side THD values were within a permissible level, which demonstrated a satisfactory overall system performance.

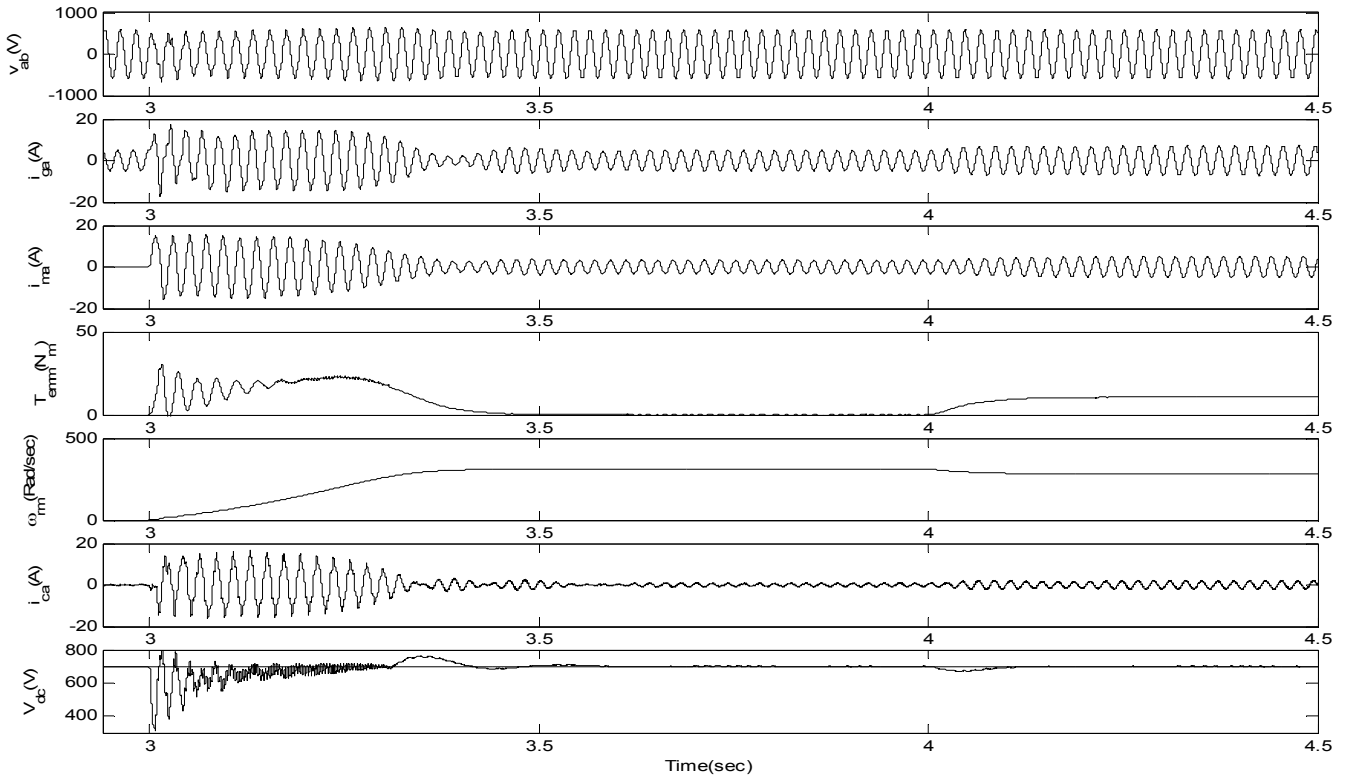


Figure 7. Performance characteristics of SEIG-STATCOM (cost-effective) with induction motor load (Load conditions:  $T_L = 0$  at 3.0 sec. and  $T_L =$  rated torque at 4.0 sec.)

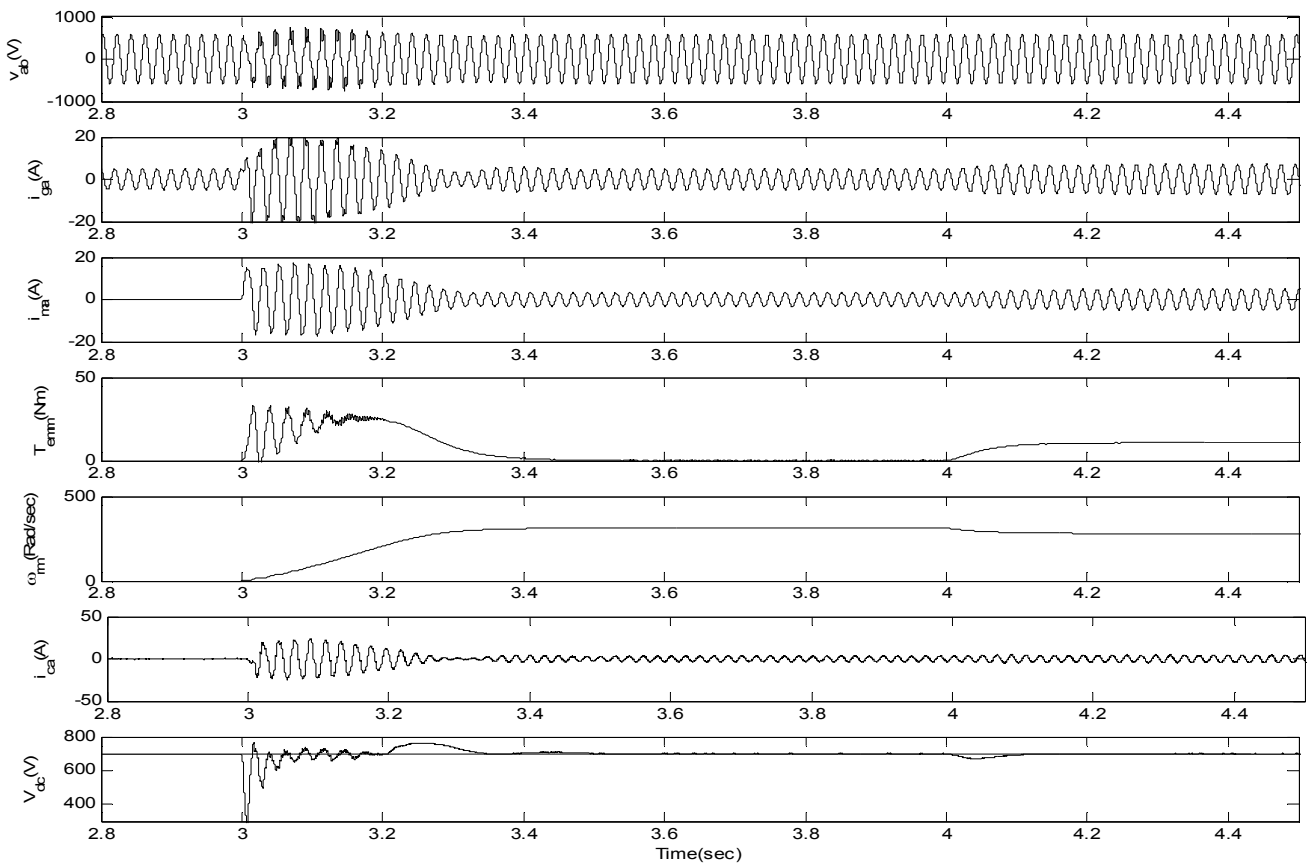


Figure 8. Performance characteristics of SEIG-STATCOM (full-rating) with induction motor load (Load conditions :  $T_L = 0$  at 3.0 sec. and  $T_L =$  rated torque at 4.0 sec.)

**Table 3.** Comparison of performance indices of the system with and without STATCOM

Performance index	Without STATCOM	With STATCOM	
		Cost-effective design	Full-rating design
Supply voltage dip at start-up	75%	10.0%	6.1%
Start-up time	0.7 sec	0.18	0.16 sec
Supply current THD at full motor load	NA	1.4%	1.3%
Rise/drop in DC bus voltage of STATCOM at the time of sudden IM loading	NA	840V/300V	790V/330V
Drop in DC bus voltage with full torque loading of IM	NA	625V	650V

## CONCLUSIONS

The investigations on SEIG-STATCOM system have been presented for feeding static R-L and induction motor loads. The dynamic model of the system has been developed in state space form. The STATCOM parameters have been calculated for two design cases, namely the cost-effective and full-rating designs using the proposed design procedure. The cost-effective STATCOM was designed to provide a stable operation by connecting additional shunt capacitance with the load. The system performance has been presented for both the cost-effective and full-rating STATCOM. With a controlling algorithm, the system exhibited improved performance in terms of parameters such as starting time, voltage dip, generator current and total harmonic distortion in the supply current under various transient conditions. The full-rating STATCOM could be considered for critical applications having stringent performance consideration while the cost-effective STATCOM should be for remote applications where the cost is important.

## Appendix I

The per phase equivalent circuit of SEIG feeding induction motor load at steady state is shown in Figure 9. In the equivalent circuit, the SEIG parameters  $R_s$  and  $X_{ls}$  are stator resistance and leakage reactance respectively,  $R_r$  and  $X_{lr}$  are rotor resistance and leakage reactance respectively, and  $X_m$  is the magnetising reactance. The corresponding parameters are presented with subscript  $m$  for motor load.  $X_{csh}$  is the reactance offered by the capacitor bank, and  $F$  and  $v$  are per unit frequency and prime-mover speed respectively.

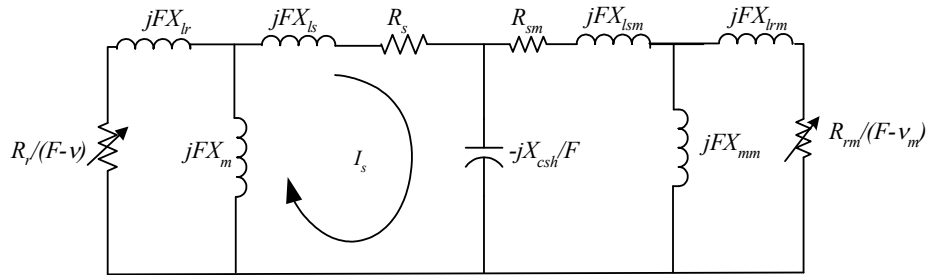


**Figure 9.** Per phase equivalent of SEIG feeding motor load

Applying KVL on stator side loop of induction generator results in

$$Z_{loop} I_s = 0$$

Under steady state condition,  $I_s$  cannot be zero and therefore  $Z_{loop}$  should be zero. An optimisation problem has been formulated to obtain the unknown variables  $X_{csh}$  and  $F$ . The objective function  $F_n$  is expressed as

$$F_n(X_{csh}, F) = abs(Z_{loop})$$

The values of  $X_{csh}$  and  $F$  should lie between the respective minimum and maximum limits:

$$(F_{mn} \leq F \leq F_{mx}), (X_{cmn} \leq X_{csh} \leq X_{cmx})$$

The above optimisation problem is solved through SUMT in conjunction with the Rosenbroack method of direct search technique [23]. After the convergence, the capacitance is computed.

## Appendix II

The induction machine model is developed in a stationary reference frame while incorporating the effects of both the main flux and cross-flux saturation. The forms of  $[v]$ ,  $[i]$ ,  $[r]$ ,  $[L]$  and  $[G]$  are given as

$$[v] = [v_{qs} \quad v_{ds} \quad v_{qr} \quad v_{dr}]^T ; \quad [i] = [i_{qs} \quad i_{ds} \quad i_{qr} \quad i_{dr}]^T ; \quad [r] = \text{diag}[r_s \quad r_s \quad r_r \quad r_r]$$

$$[L] = \begin{bmatrix} L_{sq} & L_{dq} & L_{mq} & L_{dq} \\ L_{dq} & L_{sq} & L_{dq} & L_{md} \\ L_{mq} & L_{dq} & L_{rq} & L_{dq} \\ L_{dq} & L_{md} & L_{dq} & L_{rd} \end{bmatrix} \quad [G] = \begin{bmatrix} 0 & 0 & 0 & 0 \\ 0 & 0 & 0 & 0 \\ 0 & -\omega_r L_m & 0 & L_r \\ -\omega_r L_m & 0 & L_r & 0 \end{bmatrix}$$

The air gap voltage of SEIG does not remain constant during loading. Therefore, the magnetising inductance is calculated by calculating the magnetising current as

$$i_m = \sqrt{(i_{qs} + i_{qr})^2 + (i_{ds} + i_{dr})^2}$$

The inductances in  $[L]$  are evaluated [21] as

$$L_m = \lambda_m / i_m, L = d\lambda_m / di_m, \cos \mu = i_{dm} / i_m, \sin \mu = i_{qm} / i_m$$

$$L_{dq} = (L - L_m) \cos \mu \sin \mu$$

$$L_{mq} = L \cos^2 \mu + L_m \sin^2 \mu, L_{md} = L \sin^2 \mu + L_m \cos^2 \mu$$

$$L_{sq} = L_{ls} + L_{mq}, L_{sd} = L_{ls} + L_{md}, L_{rq} = L_{lr} + L_{mq}, L_{rd} = L_{lr} + L_{md}$$

The prime mover torque driving the induction machine is expressed as

$$T_p = 6200 - 20\omega_r$$

### Appendix III

#### Generator parameters

3.7 kW, 415 V,  $\Delta$ -connected, 7.6 A (line), 50 Hz, 4 pole,  $J=0.0842$  kg-m<sup>2</sup> cage induction machine.  
 $R_s=0.0585$  pu,  $R_r=0.06196$  pu,  $X_{ls}=X_{lr}=0.1015$  pu,  $X_{m(unsat)}=2.858$  pu.

#### Magnetisation characteristic of SEIG

$$L_m = K_1 i_m^2 + K_2 i_m + K_3$$

where  $K_1 = -0.0091$ ,  $K_2 = 2.0024$ ,  $K_3 = 348.35$ .

#### Motor parameters

1.5 kW, 415 V,  $\Delta$ -connected, 3.2 A (line), 50 Hz, 4 pole,  $J=0.0205$  kg-m<sup>2</sup> cage induction machine.  
 $R_{sm}=0.0832$  pu,  $R_{rm}=0.0853$  pu,  $X_{ism}=X_{lrm}=0.1101$  pu,  $X_{mm(unsat)}=1.83$  pu.

#### Magnetisation characteristic of motor

$$L_{mm} = K_{m1} i_{mm}^5 + K_{m2} i_{mm}^4 + K_{m3} i_{mm}^3 + K_{m4} i_{mm}^2 + K_{m5} i_{mm} + K_{m6}$$

where  $K_{m1} = 0.0072$ ,  $K_{m2} = -0.0849$ ,  $K_{m3} = 0.4298$ ,  $K_{m4} = 0.9924$ ,  $K_{m5} = 0.6847$ ,  $K_{m6} = 1.171$ .

**REFERENCES**

1. S. Major, T. Commins, and A. Noppharatana, "Potential of wind power for Thailand: An assessment", *Maejo Int. J. Sci. Technol.* **2008**, 2, 255-266.
2. F. F. Li, J. Kueck, T. Rizy and T. King, "A preliminary analysis of the economics of using distributed energy as a source of reactive power supply", Report for the U.S. Department of Energy, **2006**, [www.localpower.org/documents/reporto\\_doe\\_reactivepowerandde.pdf](http://www.localpower.org/documents/reporto_doe_reactivepowerandde.pdf).
3. E. D. Bassett and F. M. Potter, "Capacitive excitation for induction generators", *AIEE Trans. (Elect. Eng.)*, **1935**, 54, 540-545.
4. J. M. Elder, J. T. Boys and J. L. Woodward, "Self-excited induction machine as a small low-cost generator", *IEE Proc. Gener. Transm. Distrib.*, **1984**, 131, 33-41.
5. S. S. Murthy, O. P. Malik and A. K. Tandon, "Analysis of self excited induction generators", *IEE Proc. Gener. Transm. Distrib.*, **1982**, 129, 260-265.
6. L. Shridhar, B. Singh, C. S. Jha and B. P. Singh, "Analysis of self excited induction generator feeding induction motor", *IEEE Trans. Ener. Convers.*, **1994**, 9, 390-396.
7. E. Bim, J. Szajner and Y. Burian, "Voltage compensation of an induction generator with long-shunt connection", *IEEE Trans. Ener. Convers.*, **1989**, 4, 526-530.
8. M. H. Haque, "Selection of capacitors to regulate voltage of a short-shunt induction generator", *IET Gener. Transm. Distrib.*, **2009**, 3, 257-265.
9. L. Wang and J. Y. Su "Effects of long-shunt and short-shunt connections on voltage variations of a self-excited induction generator", *IEEE Trans. Ener. Convers.*, **1997**, 12, 368-374.
10. S. M. Alghuwainem, "Steady-state analysis of an induction generator self excited by a capacitor in parallel with saturable reactor", *Electr. Mach. Power Syst.*, **1998**, 26, 617-625.
11. S. C. Kuo and L. Wang, "Analysis of isolated self-excited induction generator feeding a rectifier load", *IEE Proc. Gener. Transm. Distrib.*, **2002**, 149, 90-97.
12. T. L. Maguire and A. M. Gole, "Apparatus for supplying an isolated DC load from a variable-speed self-excited induction generator", *IEEE Trans. Ener. Convers.*, **1993**, 8, 468-475.
13. A. S. Yome and N. Mithulanathan, "Comparison of shunt capacitor, SVC and STATCOM in static voltage stability margin enhancement", *Int. J. Electr. Eng. Edu.*, **2004**, 41, 158-171.
14. B. Singh, K. Al-Haddad and A. Chandra, "Harmonic elimination, reactive power compensation and load balancing in three-phase, four-wire electric distribution systems supplying non-linear loads", *Electr. Power Syst. Res.*, **1998**, 44, 93-100.
15. S. K. Jain, P. Agarwal and H. O. Gupta, "Fuzzy logic controlled shunt active power filter for power quality improvement", *IEE Proc. Electr. Power Appl.*, **2002**, 149, 317-328.

16. S. M. Ramsay, P. E. Cronin, R. J. Nelson, J. Bian and F. E. Menendez, "Using distribution static compensators (D-STATCOMs) to extend the capability of voltage-limited distribution feeders", Proceedings of IEEE Rural Electric Power Conference, **1996**, Fort Worth, TX, USA, pp. A4:1-A4:7.
17. K. N. Choma and M. Etezadi-Amoli, "The application of a DSTATCOM to an industrial facility", Proceedings of IEEE Power Engineering Society Winter Meeting, **2002**, New York, USA, Vol. 2, pp. 725-728.
18. B. Singh and L. B. Shilpakar, "Analysis of a novel solid state voltage regulator for a self-excited induction generator", *IEE Proc. Gener. Transm. Distrib.*, **1998**, 145, 647-655.
19. S. C. Kuo and L. Wang, "Analysis of voltage control for a self-excited induction generator using a current-controlled voltage source inverter (CC-VSI)", *IEE Proc. Gener. Transm. Distrib.*, **2001**, 148, 431-438.
20. B. Singh, S. S. Murthy and S. Gupta, "Analysis and design of STATCOM-based voltage regulator for self-excited induction generators", *IEEE Trans. Ener. Convers.*, **2004**, 19, 783-790.
21. E. Levi, "Applications of the current state space model in analyses of saturated induction machines", *Electr. Power Syst. Res.*, **1994**, 31, 203-216.
22. P. C. Krause, "Analysis of electrical machinery", McGraw Hill, New York, **1986**.
23. S. S. Rao, "Engineering optimization, theory and practice", New Age International, New Delhi, **1998**.